



Article

ROS-Responsive PLGA-NPs for Co-Delivery of DTX and DHA for Colon Cancer Treatment

Roberta Cassano ^{1,†}, Sonia Trombino ^{1,†}, Federica Curcio ¹, Roberta Sole ¹, Gabriella Calviello ^{2,3,*},
and Simona Serini ^{2,3,*}

¹ Department of Pharmacy, Health and Nutritional Sciences, University of Calabria, Arcavacata di Rende, 87036 Cosenza, Italy; roberta.cassano@unical.it (R.C.); sonia.trombino@unical.it (S.T.); federica.curcio@unical.it (F.C.); roberta.sole@unical.it (R.S.)

² Department of Translational Medicine and Surgery, Section of General Pathology, School of Medicine and Surgery, Università Cattolica del Sacro Cuore, Largo F. Vito, 00168 Rome, Italy

³ Fondazione Policlinico Universitario A. Gemelli IRCCS, Largo F. Vito, 00168 Rome, Italy

* Correspondence: gabriella.calviello@unicatt.it or gabriella.calviello@gmail.com (G.C.); simona.serini@unicatt.it (S.S.)

† These authors contributed equally to the work.

‡ These authors contributed equally to the work.

Abstract: The aim of this work was to evaluate the antineoplastic effect of newly synthesized nanoparticles based on poly(lactic-co-glycolic acid) (PLGA) alone or PLGA esterified with 2,2'-[propane-2,2-diylbis (thio)] diacetic acid (TKL), loaded with docetaxel (DTX) and/or docosahexaenoic acid (DHA), as innovative site-specific therapeutic carriers. The obtained materials were characterized by FT-IR and ¹H-NMR, while the dimensional analysis of the nanoparticles obtained was performed by Dynamic Light Scattering. The encapsulation efficiency of the nanoparticles was evaluated, and in vitro skin permeation tests were also performed. The antitumor activity of the nanomaterial was studied in the human adenocarcinoma HCT116 cell line. In particular, viability tests in bidimensional culture, as well as in tumor spheroids, were conducted. The use of these nanocarriers could facilitate the stable and efficient delivery of DTX and DHA through the upper segments of the gastrointestinal tract to the colon. In addition, the presence of the ROS-sensitive 2,2'-[propane-2,2-diylbis (thio)] diacetic acid in their matrix should promote the site-specific release of DTX in the tumor mass, where high levels of reactive oxygen species could be found.

Keywords: colon cancer; docosahexaenoic acid; docetaxel; nanoparticles; PLGA; 2,2'-[propane-2,2-diylbis (thio)] diacetic acid; tumor spheroids



Citation: Cassano, R.; Trombino, S.; Curcio, F.; Sole, R.; Calviello, G.; Serini, S. ROS-Responsive PLGA-NPs for Co-Delivery of DTX and DHA for Colon Cancer Treatment. *Int. J. Transl. Med.* **2024**, *4*, 262–277. <https://doi.org/10.3390/ijtm4020016>

Received: 18 March 2024

Revised: 19 April 2024

Accepted: 22 April 2024

Published: 25 April 2024



Copyright: © 2024 by the authors. Licensee MDPI, Basel, Switzerland. This article is an open access article distributed under the terms and conditions of the Creative Commons Attribution (CC BY) license (<https://creativecommons.org/licenses/by/4.0/>).

1. Introduction

Colorectal cancer (CRC) represents the second most frequently diagnosed cancer and ranks as the fourth leading cause of cancer-associated death on a global scale [1]. It begins with the formation of polyps on the internal surface of the mucosa and then gradually begins to progress, invading the colorectal tissues and causing symptoms such as intestinal bleeding, constipation and severe abdominal pain [2]. The survival of the affected patients is especially related to the high degree of tumor recurrence and the propensity that CRC has for distant metastases [3]. Presently, conventional (such as surgery, radiotherapy and chemotherapy) or innovative (targeted therapy and immunotherapy) anticancer therapies are applied for this kind of cancer [3,4]. Particularly, chemotherapy still represents the predominant form of therapy in patients experiencing recurrence, as well as in the advanced form of this cancer [5]. However, as CRC is still linked to significant morbidity and mortality, a great deal of investigations are currently ongoing to find new diagnostic and therapeutic approaches [6]. The new therapeutic strategies in this field are especially aimed to provide higher drug concentration in the colon and fewer systemic

side effects [7,8], and drug delivery systems such as nanoparticles (NPs) are considered particularly promising in this respect [9,10]. Moreover, since chemotherapy is still mostly administered parenterally, which represents a discomfort for the patient, oral administration of the NPs is considered a desirable therapeutic approach, especially for chronic patients requiring long-term treatment [6,11]. Of interest, NPs seem to be particularly promising for the development of an oral formulation for CRC, since they could protect the drugs from destructive effects during the passage through the gastrointestinal tract [12] and thus allow higher local concentrations to reach the affected colorectal tissues.

On these bases, our main aim here was to develop a nanoformulation for oral administration able to deliver docetaxel (DTX) efficiently and specifically to CRC cells and, thus, avoid the dangerous side effects usually observed with this drug in clinical practice. Our choice was related to the fact that this antineoplastic agent belonging to the taxane family [13] is known to exert powerful antitumor effects against a variety of human cancers, including cervical cancer, prostate cancer, non-small-cell lung cancer, breast cancer and leukemia [14]. It acts by inducing depolymerization of microtubules resulting in an arrest of cells in the G2/M phase of the cell cycle and cell death [15]. However, even though its anticancer potential is so high for other cancers, its efficiency in the treatment of CRC cancer is quite limited [16,17]. On these bases, recently, considerable efforts have been expended in trying to enhance the antineoplastic activity of DTX and other taxanes toward CRC and construct highly potent next-generation taxanes with enhanced anti-neoplastic capacities, which could be extremely important for the therapy of CRC, since it, differently from other cancers, hardly responds to immunotherapy with checkpoint inhibitors [18–20]. One of the explored strategies is that of combining the treatment with DTX with that of other antineoplastic agents [21,22]. One possible combination strategy that has been largely explored in breast cancer and has been shown to induce a considerable increase in the DTX antineoplastic efficacy is the combined treatment of DTX with omega-3 polyunsaturated fatty acids (PUFAs) and, in particular, with the long-chain omega-3 PUFA docosahexaenoic acid (DHA, 22:6 n-3) [23–25] which is a natural compound present in our diet. It is incorporated at high levels in our cellular membranes and is devoid of side effects [26]. We here hypothesized that omega-3 PUFAs could have this potentiating activity toward DTX also in CRC. In fact, the antineoplastic effects of these fatty acids are well known and include the induction of apoptosis, autophagy and inhibition of cell proliferation by a series of different mechanisms, among which the modulation of the cell membrane lipid composition, which, in turn, may alter the content and the functions of transmembrane proteins and signaling transduction pathways [27–32]. Moreover, these omega-3 PUFAs are well known for their anti-inflammatory activity [33–37]. In particular, we have previously found that they have the capacity to reduce the growth of CRC cells *in vitro* by regulating some crucial molecular mechanisms involved in CRC cell growth and survival [38–41] and to overcome their resistance to 5-FU chemotherapy [42], as well as to reduce tumor-induced neoangiogenesis [43].

In addition, it should be underlined that the use of DTX is related to a series of side effects, such as acute hypersensitivity, hypotension, fluid accumulation, myelosuppression, neutropenia, peripheral neurotoxicity, epithelial necrosis, vomiting and diarrhea [13]. In the DTX intravenous formulations currently available for clinical use, the drug is dissolved in ethanol and Tween 80, due to the scarce solubility of the drug in water. However, the presence of Tween 80 in the available nanoformulations was reported to cause peripheral neuropathy [44,45] as well as severe hemolysis [46]. In this respect, there exists extensive research demonstrating that omega-3 PUFAs, due to their powerful anti-inflammatory and immunomodulating activities [34–37], are able to reduce multiple side effects caused by chemotherapeutic treatments in the clinical practice and for all kinds of cancers, including gastrointestinal cancers [47,48].

To construct our nanoformulation, we used here poly(lactic-co-glycolic acid) (PLGA), a physiologically biocompatible and biodegradable polymer, which is synthesized as a copolymer of lactic and glycolic acid at various monomer ratios. We conjugated PLGA with

2,2'-[propane-2,2-diylbis (thio)] diacetic acid (TKL), which is a linker capable of forming ester bonds that can be cleaved by high levels of reactive oxygen species (ROS) [49]. Thus, the presence of this ROS-sensitive linker in the NP matrix could favor the site-specific release of DTX in the colonic mucosa area. In fact, the tumor microenvironment is particularly rich in ROS, which are known for their capacity to promote cancer development and progression [50]. All materials were characterized by FT-IR, ¹H-NMR and Dynamic Light Scattering, and the encapsulation efficiency of the NPs was assessed. In addition, *in vitro* skin permeation was performed to establish whether the new formulations improved drug skin penetration. Moreover, antitumor activity tests on the human colon adenocarcinoma HCT116 cell line were conducted. In particular, the effect of the NPs on the viability of the CRC cells was analyzed. Furthermore, the antineoplastic activity of the NPs was assessed through the evaluation of the proliferation of the HCT116 cell-derived spheroids. In fact, recently, increasing importance has been given to the evaluation of the antineoplastic effects in three-dimensional models (3D), such as the spheroids obtained by cultured tumor cells, which mimic in a more realistic way the growth conditions of tumor cells *in vivo* [51].

2. Materials and Methods

2.1. Materials

For the synthesis processes, the following materials were used: N,N-dicyclohexylcarbodiimide (DCC), 4-dimethylaminopyridine (DMAP) and dimethylsulfoxide (DMSO) (purchased from Sigma-Aldrich, St. Louis, MO, USA); PVA was purchased from Polysciences (Badener, Germany), poly(lactic-co-glycolic acid) (PLGA), DHA and Docetaxel (DTX) were purchased from Sigma-Aldrich (St. Louis, MO, USA), and 2,2'-[propane-2,2-diylbis(thio)]diacetic acid (TKL) was purchased from BLD Pharmatech (Kaiserslautern, Germany). The solvents used were dichloromethane (purchased from VwR Chemicals Prolabo) and acetone (purchased from LabScan Analytical Sciences, Gliwice, Poland).

2.2. Instrumentation

FT-IR spectra were recorded using a Jasco 4200 spectrophotometer (Cremella, Italy), ¹H-NMR spectra were recorded using a Bruker VM 30 spectrophotometer (Milano, Italy), and UV-vis spectra were recorded using a Jasco V-530 UV/Vis spectrophotometer (Cremella, Italy). Size analysis of the polymer nanoparticles was carried out by light scattering using a Brookhaven 90 Plus Particle Size Analyzer (New York, NY, USA), while solvent removal was performed using a Rotavapor R II, Buchi (Cornaredo, Italy). Freeze-drying of some compounds was performed through an Edwards MicroModule Freeze dryer (Cheshire, UK). Silica gel plates on aluminum from Merck (Serono, Italy) were used for thin-layer chromatography. The sonicator (DK Sonic, Shenzhen, China) was used to increase the solubilization of the samples in acetone; centrifugation was carried out using the centrifuge (Rodano, MI, Italy), which was used in order to have a good separation between precipitate and supernatant, taking advantage of the centrifugal acceleration.

2.3. Synthesis of the PLGA-2,2'-[Propane-2,2-diylbis (thio)] Diacetic Acid Ester

In a three-necked flask, fitted with a reflux condenser, 0.043 g (0.19 mmol) of 2,2'-[propane-2,2-diylbis (thio)] diacetic acid, 0.08 g of DCC (0.38 mmol), 0.001 g of dimethylaminopyridine (8.18×10^{-6} mmol) and 0.063 g (0.38 mmol) of PLGA were added to 150 mL of dichloromethane. The flask was placed under magnetic stirring for 48 h at room temperature. The course of the reaction was followed by thin-layer chromatography of a chloroform/hexane eluent mixture (5:5). The resulting product (ester) was purified by filtration and washing in hot methanol to remove the residual dicyclohexylurea (DCU), i.e., the condensation reaction by-product of DCC with amines and alcohols, formed and the remaining solvent residue [52,53].

2.4. Nanoparticle Realization

Nanoparticles (NPs) were synthesized by the nanoprecipitation technique using a water-acetone system. Specifically, the obtained ester (PLGA+TKL) or PLGA alone (in the presence or absence of the drugs) was solubilized in acetone (1.25 mL) under magnetic stirring. Subsequently, a 4% (*w/v*) solution of polyvinyl alcohol (PVA) in water was added. The reaction was kept under agitation for about 10 min, and the acetone was subsequently removed under reduced pressure [54,55]. The obtained nanoparticles were washed three times in water and centrifuged at 9100 rpm for 20 min. The precipitate obtained was resuspended in water and lyophilized. Drug-loaded nanoparticles were prepared by the same procedure as empty ones, solubilizing either docetaxel and ester (PLGA+TKL) or docetaxel and PLGA in acetone. The quantities of substrates and docetaxel are shown in Table 1.

Table 1. Amounts of substrates used.

Nanoparticles	PLGA (g)	PLGA+TKL (g)	DHA (g)	DOCETAXEL (g)
Empty PLGA-NPs	0.0025	-	-	-
Empty PLGA-TKL-NPs	-	0.005	-	-
PLGA-DTX-DHA NPs	0.0025	-	0.00025	0.001
PLGA-TKL-DTX NPs	-	0.005	-	0.001

2.5. Evaluation of Encapsulation Efficiency

The encapsulation efficiency was evaluated by UV-vis spectrophotometry. The nanoparticles were solubilized in a 10% acetone solution and sonicated for 30 min at 37 °C to facilitate their rupture and the escape of the encapsulated drugs. After centrifugation for 20 min at 4000 rpm, the supernatants were resuspended with 1 mL of PBS + EtOH (7:3) and were analyzed on a UV-vis spectrophotometer ($\lambda_{DHA} = 233$ nm and $\lambda_{DTX} = 273$ nm A). The rupture method was employed for both drug-loaded and empty nanoparticles, with the empty nanoparticles used as a blank control for the loaded nanoparticle absorbance reading. The encapsulation efficiency was then determined using the following equation:

$$EE\% = \frac{gf}{gi} \times 100$$

where *gi* indicates the initial drug concentration, and *gf* indicates the actual amount trapped in the nanoparticles.

2.6. In Vitro Drug Release Studies

Skin permeation studies were performed by the dialysis method using semi-synthetic cellulose acetate membranes with a 12 kDa cut-off. Specifically, the nanoparticles obtained (empty and full) were placed inside the membranes and immersed in a solution consisting of PBS + EtOH (7:3) at pH 7.4 and maintained at a temperature between 35.5 and 37.5 °C, in order to mimic physiological conditions. At regular time intervals (30 min, 1 h, 2 h, 4 h, 6 h, 12 h, 24 h), 2 mL of solution was withdrawn and replaced with fresh release solution to maintain the same total volume during the study. Samples were analyzed by UV-vis spectrophotometry ($\lambda_{DHA} = 233$ nm and $\lambda_{DTX} = 273$ nm A), and drug release profiles were expressed as the percentage of drug released relative to the total amount loaded as a function of time.

2.7. Evaluation of Antitumor Activity

The colon adenocarcinoma cell line HCT116 was obtained from the American Type Culture Collection (ATCC, Manassas, VA, USA). The cells were maintained in DMEM culture medium containing glutamine (2 mM), antibiotics (Penicillin 100 U/mL, Streptomycin

100 µg/mL), sodium pyruvate, non-essential amino acids and fetal bovine serum (FBS, 10%) at 37 °C in a humidified atmosphere with 5% CO₂. The cells were maintained in exponential growth phase by seeding them twice a week at a concentration of 3 × 10⁵ cells/mL. Freeze-dried particle samples (NPs) based on only PLGA or PLGA+TKL and containing or not DTX (10%) or a combination of DTX (5%) and DHA (5%) were resuspended directly in the culture medium at a concentration of 1 mg/mL. Aliquots of 5 µL/mL and 10 µL/mL for each stock solution were used to treat cells in cytotoxicity experiments.

2.8. Cell Viability Assessment by In Vitro MTT Assay

The MTT assay was used to assess cellular metabolic activity as an indicator of cell viability. This colorimetric method is based on the reduction of the tetrazolium salt 3-(4,5-dimethylthiazol-2-yl)-2,5-diphenyltetrazolium bromide (or MTT), which is a yellow-colored compound, to violet blue-colored formazan crystals by metabolically active cells. Viable cells contain the mitochondrial enzyme succinate dehydrogenase, which converts the tetrazolium ring of MTT (yellow) to formazan (violet blue). The insoluble formazan crystals are dissolved using dimethyl sulfoxide (DMSO), and the resulting colored solution is quantified by measuring the absorbance at 570 nm [56]. The greater the staining of the solution, the greater the number of metabolically active viable cells.

HCT116 cells were seeded at a concentration of 5 × 10³ cells/well in a 96-well multi-well plate at a final volume of 200 µL/well. After 24 h, the culture medium was removed and replaced with fresh medium containing or not empty PLGA-based nanoparticles (PLGA-NPs) and containing TKL (PLGA-TKL NPs) in the absence or presence of 10% DTX (PLGA-TKL-DTX-NPs) or a combination of DHA and DTX (both 5%) (PLGA-DTX-DHA-NPs) at a concentration of 5 µL/mL and 10 µL/mL. The cells were also treated with pure DHA (0.75 µM and 1.5 µM, the same concentration present in the two different concentrations of PLGA-DTX-DHA-NPs, starting from a 1 mM stock solution in pure ethanol) and with pure DTX (at the concentration of 0.61 µM and 1.24 µM, the concentrations of the drug present in the two different concentrations of PLGA-TKL-DTX-NPs) starting from a 1 mM stock solution of the drug in DMSO. At increasing time points (24, 48 and 72 h), 50 µL of MTT solution (2 mg/mL in PBS) was added inside each well, and the culture plate was further incubated at 37 °C for 4 hours. Subsequently, the supernatant was removed, and the formed formazan crystals were solubilized using DMSO (100 µL/well). Absorbance was measured at 570 nm and 630 nm (as basal absorbance to be subtracted from that evaluated at 570 nm) using a plate spectrophotometer (Tecan, Männedorf, Switzerland). Cell viability was calculated using the following formula:

$$\% \text{ cells viability} = \frac{\text{Absorbance of treated cells}}{\text{Absorbance of control cells}} \times 100$$

2.9. Spheroid Cell Viability In Vitro

To obtain the spheroids, we used commercially available cell culture plates (Biomimesys[®] 3D Cell Culture Hydroscaffold[™], HCS Pharma, Loos, France), providing a microenvironment that reproduces all the characteristics of human tissues, including the matrix architecture, the cell organization and cell–cell and cell–matrix interactions. The matrix of Biomimesys[®] culture plates consists of hyaluronic acid, the main glycosaminoglycane of extracellular matrix, collagen and adhesion molecules. The concentration of cell suspension was calculated in order to seed the cells on the matrix at a volume of 30 µL/well (as indicated by the manufacturer to obtain the maximum penetrance of cells within the matrix). Culture medium was then added to a final volume of 200 µL/well. Culture medium was changed each other day until the sixth day (the time after which the formation of tumor cell spheroids was well visible with the microscope). Then, cell culture medium was gently removed with a pipette tip and replaced with fresh culture medium containing or not empty PLGA-based nanoparticles (PLGA-NPs) and containing TKL (PLGA-TKL NPs) in the absence or presence of 10% DTX (PLGA-TKL-DTX-NPS) or a combination of DHA and DTX (both 5%) (PLGA-DTX-DHA-NPs) at a concentration of 5 µL/mL. Also in this

experiment, the spheroids were treated with pure DHA (0.75 μM) and with pure DTX (0.62 μM). After 72 h, the spheroid viability was evaluated by using a commercial colorimetric kit (3D Culture HTS Cell Viability Assay Kit, Abcam, Cambridge, UK), following the manufacturer's instructions. Briefly, after treatment, cell culture medium was removed, and 200 μL of matrix dissociation salt solution was added to each well. Culture plate was then incubated at room temperature for 10 min, and the matrix was dissociated by using a 1 mL pipette tip. A total of 50 μL of Viability Assay buffer was added into each well, and the culture plate was centrifuged at $100\times g$ for 5 min at 4 $^{\circ}\text{C}$. The supernatant was gently removed, and the cells were resuspended in 150 μL of fresh Viability Assay buffer. At the same time, a standard curve was prepared using the same cell type (HCT116). Cells were trypsinized, resuspended in a small volume of Viability Assay buffer and counted. A cell suspension was prepared at the concentration of 2.5×10^6 cells/mL. Then, aliquots of 0, 5, 10, 20, 30 and 100 μL of cell suspension (corresponding to 12,500, 25,000, 50,000, 75,000, 125,000 and 250,000 cells, respectively) were put into the wells of a different 96-well culture plate in duplicate, and the volume in the single wells was adjusted to 150 μL of Viability Assay buffer. In all the wells (samples and standard curve), 50 μL of WST staining was added. Culture plates were incubated at 37 $^{\circ}\text{C}$, and at increasing time points (30, 60, 90, 120, 150 and 180 min), spectrophotometric evaluation was performed at the wavelength of 460 nm using a plate spectrophotometer (Tecan, Männedorf, Switzerland) in order to establish the better incubation time. The viability of spheroids was calculated based on the absorbance values obtained for the standard curve.

2.10. Statistical Analysis

Data in Figures 5 and 6 were analyzed by one-way analysis of variance (ANOVA) followed by Tukey's test.

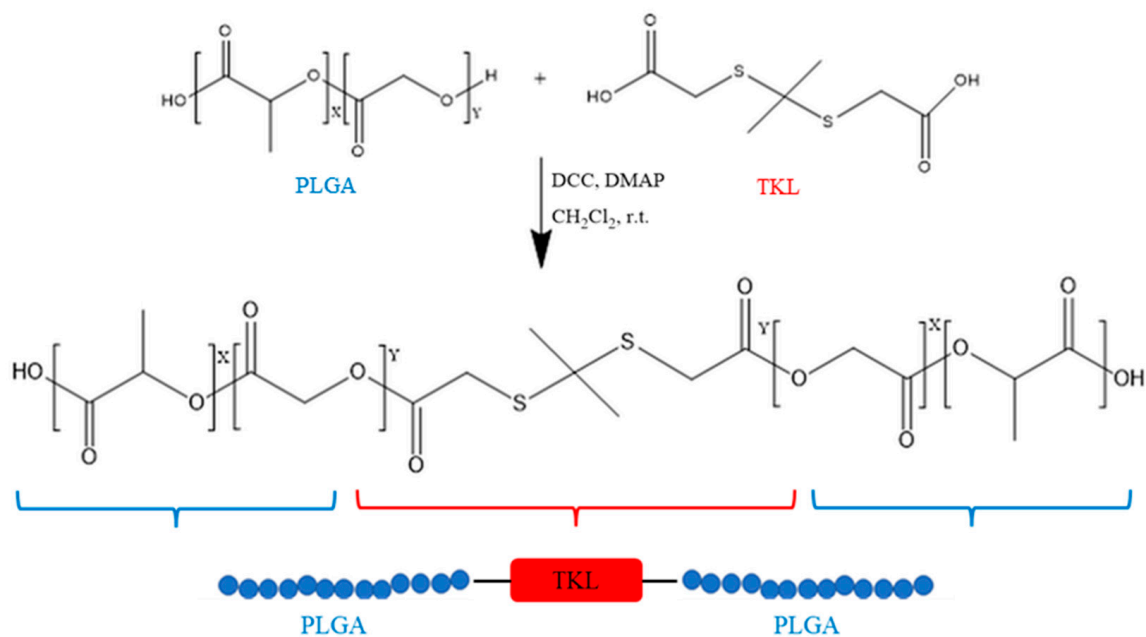
3. Results and Discussion

The different nanoparticles were produced taking into consideration previous works [18,57]. In particular, Ünal et al. fabricated nanoparticles using PLGA and also the drug DTX. By comparing the nanoparticle characterization tests, similar dimensions were observed. The size of their particle ranged from 200 nm to 300 nm. In the present work, the ROS-sensitive activity is obtained through the presence of TKL, a ROS labile linker, which has been used to functionalize the PLGA polymer matrix. This strategy was previously employed by Wang et al. [22] but using a different material: N1-(4 poly (vinyl alcohol) (PVA) linked with the ROS-labile linker: N1-(4-boronobenzyl)-N3-(4-boronophenyl)-N1,N1,N3,N3-tetramethylpropane-1,3-diaminium (TSPBA).

3.1. Synthesis and Characterization of the Ester

The esterification reaction between PLGA and TKL was conducted in dichloromethane at room temperature in the presence of N,N-dicyclohexylcarbodiimide (DCC) and 4-dimethylaminopyridine (DMAP) to obtain the final product PLGA linked with TKL (PLGA+TKL) to be used as a polymer matrix for the NPs (Scheme 1).

PLGA+TKL formation was confirmed by the FT-IR spectrum (Figure 1). In particular, in the FT-IR spectrum of PLGA (Figure 1, Panel a), stretching vibrations of the aliphatic CHs are observed at 3023 and 2949 cm^{-1} . The carbonyl group of PLGA absorbs at 1755 cm^{-1} while the carbonyl group of PLGA+TKL absorbs at 1729 cm^{-1} (Figure 1, Panel b). Stretching vibrations attributable to the CS bonding of TKL in the region between 700 and 600 cm^{-1} are also visible.



Scheme 1. Ester synthesis of PLGA and TKL.

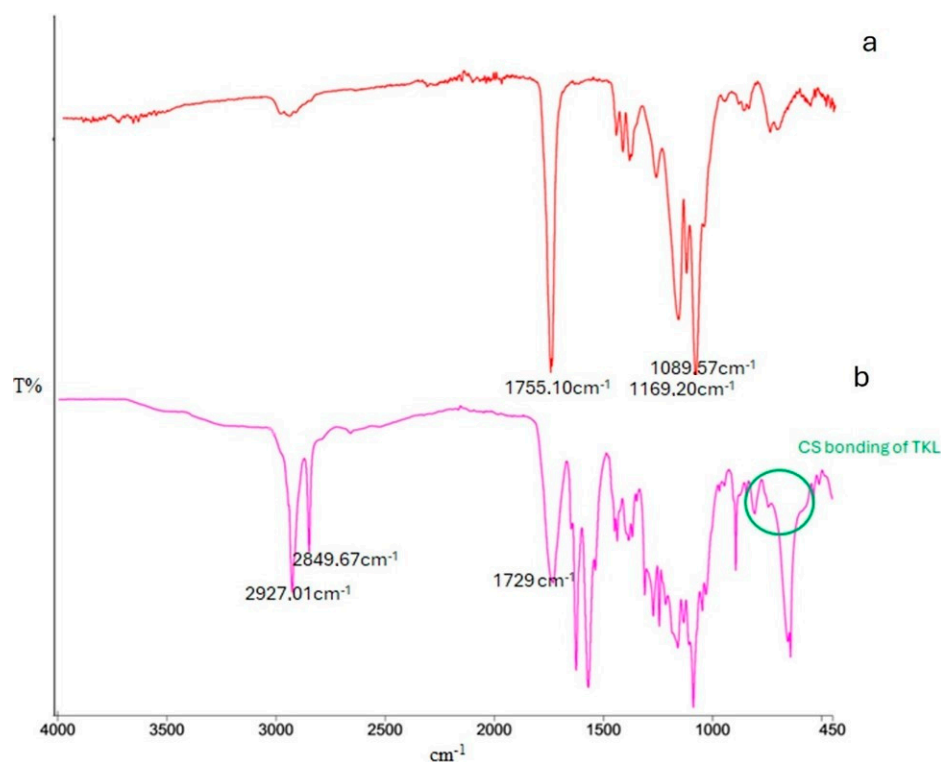


Figure 1. FT-IR analysis of PLGA (a) and PLGA+TKL (b).

The $^1\text{H-NMR}$ spectrum (Figure 2a) displays well-distinguishable signals that are attributable to the resonances of all CH_3 proton spin systems (1.2 and 1.7 ppm). The resonance of dimethylsulfoxide (DMSO) is centered at 2.51 ppm and used as the solvent for the spectral analysis. The resonance of water protons (at 3.30 ppm, in DMSO samples) could not be appreciable in the spectrum we recorded, due to the overlapping of the signals appearing at 3.36 and 3.45 ppm, which are attributable to both SCH_2 groups of the TKL linker. The signal displayed at 4.09–4.11 ppm is attributable to the CH of the lactic acid unit. The signal at 4.91 ppm is due to the OCH_2 methyl of the glycolic acid unit, and

The mean diameter of the nanoparticles and their polydispersion index (PI), analyzed by Dynamic Light Scattering, are shown in Table 2. As evident from the table, the nanoparticle sizes are comparable to each other. Surprisingly, PLGA-based nanoparticles containing the drugs DTX and DHA have small dimensions, probably due to the interactions established between the two active ingredients and the polymer matrix containing PLGA alone. The only nanocarrier with significantly larger dimensions is the one containing the PLGA, linker and docetaxel. The polydispersity index is not low, as nanoparticles tend to aggregate.

Table 2. Average particle size and PI index of empty and loaded nanoparticles.

Nanoparticles	Dimensional Analysis (nm)	Polydispersion Index (PI)
Empty PLGA NPs	218.6 ± 8.3	0.384
Empty PLGA-TKL NPs	209.7 ± 13.5	0.330
PLGA-DTX- DHA NPs	195.1 ± 183.9	0.174
PLGA-TKL-DTX NPs	856.3 ± 4.0	0.254

3.3. In Vitro Drug Release Studies

All types of NPs were also subject to the release studies of the DTX and DHA encapsulated in them, through the dialysis method using semi-synthetic membranes in cellulose acetate. A solution consisting of phosphate buffer/ethanol was used as a solvent in which ethanol acts as a co-solvent to increase the aqueous solubility of DTX and DHA. As can be seen in Figure 3, the encapsulated drugs are released from the NPs within 24 h, in quantities of about 35% of the total loaded quantity (0.064 mg) for ester-based NPs containing DTX and approximately 80% for PLGA-based NPs containing both DTX and DHA. In the latter case, the release rates were summed to obtain a single trend of DHA and DTX in Figure 3. Figure 4, on the other hand, specifically shows the release profiles of the substances (DHA and DTX) in PLGA nanoparticles. The graph shows a constant release of both substances but with a higher release of DTX than DHA.

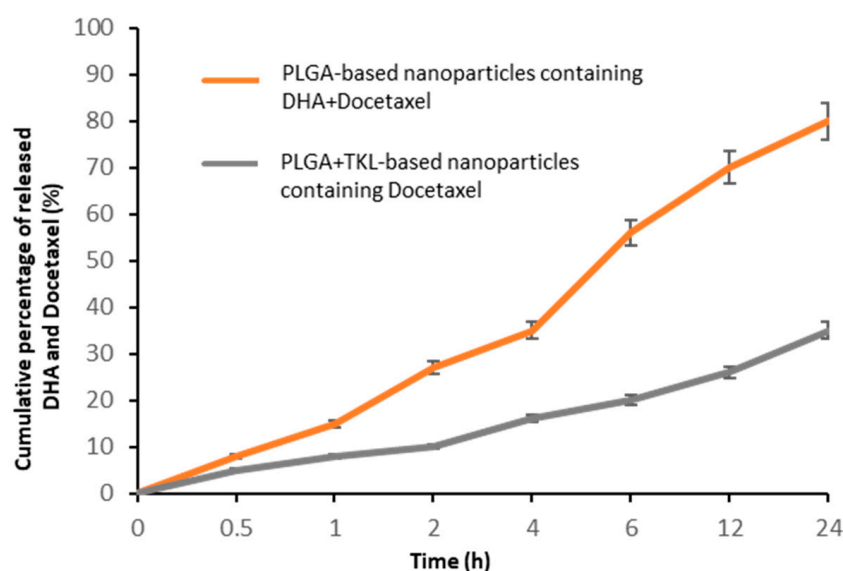


Figure 3. Drug release profile evaluated within 24 h.

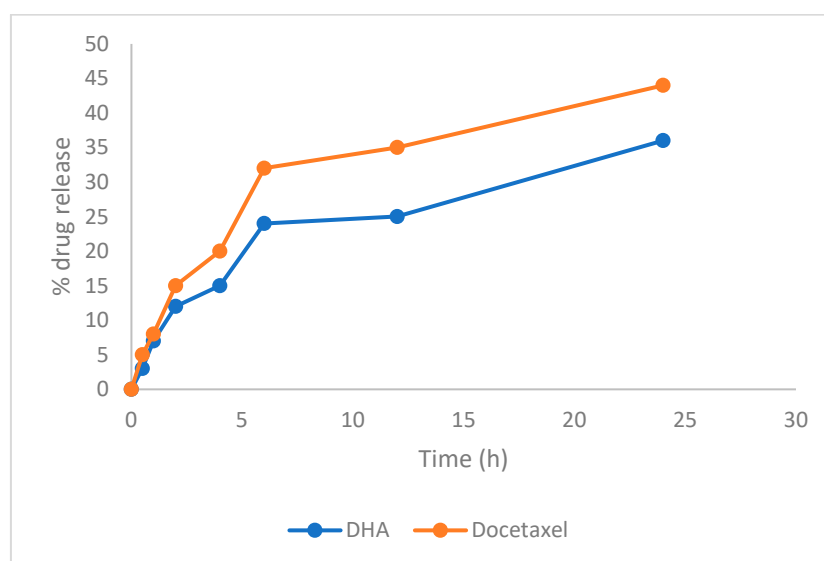


Figure 4. Drug release profile of DHA and docetaxel in PLGA nanoparticles.

3.4. Antitumor Activity Evaluation

The potential antineoplastic effect of nanoformulations was evaluated using the human colon adenocarcinoma cell line (HCT116). The mechanism of action of DTX involves its interference with mitosis [58]. Indeed, the binding of DTX to tubulin promotes the polymerization of tubulin in microtubules and prevents its disassembly [59,60]. This leads to a cell cycle arrest in the G2/M phase and then to cell death [15]. Figure 5 shows the effect of a treatment with two different concentrations of PLGA-based NPs loaded or not with TKL, containing DTX (10%) alone or in combination with DHA (5% DTX and 5% DHA). The effect of the different NPs was also compared to that exerted by the pure DTX (0.61 and 1.24 μM , corresponding to the concentrations of the drug present in the PLGA-TLK-DTX-NPs used at 5.0 $\mu\text{L}/\text{mL}$ and 10 $\mu\text{L}/\text{mL}$ in cell culture medium) and pure DHA (0.75 μM and 1.5 μM , corresponding to the concentrations of the fatty acid in the PLGA-DTX-DHA NPs used at 5.0 $\mu\text{L}/\text{mL}$ and 10 $\mu\text{L}/\text{mL}$). Firstly, in this experiment, we mainly wanted to assess the difference in the effect of NPs containing DTX alone versus that obtained by also using DHA as a potential adjuvant agent. The results obtained showed that a 24 h treatment with the pure DTX, at both concentrations used (0.61 μM and 1.24 μM), did not alter cell viability or even increase it. Only after 72 h of treatment did both DTX concentrations significantly reduce cell viability by about 20% ($p < 0.05$). Pure DHA, at both concentrations used (0.75 μM and 1.5 μM), did not significantly alter cell viability at all the time points. It should be noticed that the concentrations of DHA used in this study are extremely low compared to those (5–40 μM) usually found able to significantly reduce the viability of different human colon cancer cells [42]. Recently, it was found that DHA reduced the viability of HCT116 CRCs in the range of 20–160 μM [61]. Both DTX/DHA combinations used (0.61 μM DTX/0.75 μM DHA and 1.24 μM DTX/1.5 μM DHA) were able to clearly and significantly inhibit HCT116 cell viability only after 72 h of treatment. The enclosure of DTX and DHA into the PLGA-NPs made them extremely more efficacious in reducing the viability of HCT116 cells with respect to the combination of the pure compounds, especially at the highest concentration used (10.0 $\mu\text{L}/\text{mL}$, corresponding to 1.5 μM DHA and 1.24 μM DTX). This finding suggests that the enclosure of DHA in the PLGA-NPs may protect the fatty acid from degradation and help it to reach intact cancer cells, thus allowing very low concentrations of it to be effective against the cancer cells. It should be underlined that the empty PLGA-NPs did not reduce significantly cell viability at any concentration (5.0 $\mu\text{L}/\text{mL}$ and 10.0 $\mu\text{L}/\text{mL}$) and at any time point, demonstrating that this nanoformulation per se is not able to exert any cytotoxic effect.

Then, we decided to evaluate if the inclusion of TKL into the DTX-containing PLGA-NPs could enhance the anticancer properties of this drug (Figure 5). In fact, it was previously hypothesized by Wang et al. [22] that nanoformulations based on ROS-responsive compounds could more efficiently reach and release the drug to tumor cells. This is related to the high ROS production by tumor cells in their microenvironment [62]. The loading of the ROS-sensitive compound TKL into the PLGA-NPs induced a slight but significant reduction (ranging from 20% to 40% at the different time points, $p < 0.05$) of CRC cell viability that was observed only when used at the highest concentration (10.0 $\mu\text{L}/\text{mL}$). Interestingly, the addition of DTX to these NPs was able to further enhance the inhibitory effect on cancer cell viability, especially at 24 h of treatment and at both concentrations used (about 70% vs. control cells and 44% and 31% vs. the respective empty PLGA-TKL-NPs, $p < 0.05$). These findings further support the hypothesis that the inclusion of chemotherapeutic drugs into ROS-sensitive nanoformulations could substantially enhance their anticancer activity.

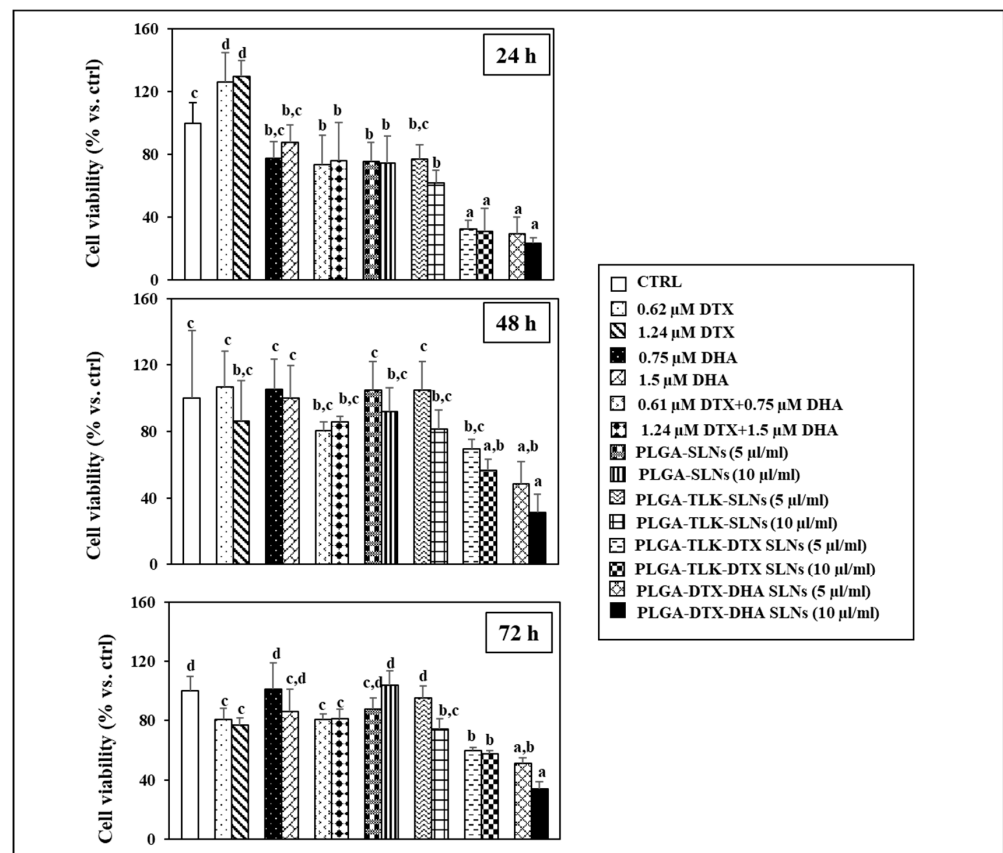


Figure 5. Effect on cell viability assessed with MTT assay (see Materials and Methods section for further details) of a treatment with two different concentrations (5 $\mu\text{L}/\text{mL}$ and 10 $\mu\text{L}/\text{mL}$) of PLGA-based empty NPs or PLGA-TKL-based empty NPs containing or not 10% DTX (corresponding to 0.62 μM and 1.24 μM) or DTX+ DHA (both at 5%, corresponding to 0.31 μM and 0.75 μM , respectively) and with pure DTX (0.61 μM and 1.24 μM) and DHA (0.75 μM and 1.5 μM). Data are means \pm SD of two different experiments performed in triplicate. Values not sharing same superscript letter are significantly different ($p < 0.05$, one-way ANOVA followed by Tukey's test).

Since spheroids mimic the growth conditions of tumor cells *in vivo* in a more realistic way with respect to a bidimensional cell culture model, we also analyzed the effects of the synthesized nanomaterials in the spheroids obtained from HCT116 cells after six days of culture in the Biomymesis[®] 96-well plates coated with a matrix consisting of hyaluronic acid, collagen and adhesion molecules and treated for further 72 h with PLGA- or PLGA-TLK-based empty NPs, PLGA-TLK-DTX or PLGA-DTX-DHA NPs. Moreover, we also treated spheroids with pure DTX at the concentration of 0.62 μM (the same amount of the

drug present in the PLGA-TLK-DTX-NPs) and with pure DHA ($0.75 \mu\text{M}$, the same amount present in the PLGA--DTX-DHA NPs), in order to verify the different effects of DTX and DHA if delivered as pure compounds or by the nanoformulations.

As can be observed in Figure 6 (panel A), when spheroids were treated with pure DTX ($0.62 \mu\text{M}$), not only did the drug not inhibit their proliferation but even increased it (+57%, $p < 0.05$). When spheroids were treated with pure DHA ($0.75 \mu\text{M}$), a slight but not significant tendency to inhibit the viability of the spheroids was observed (inhibition of 16% vs. control). However, as already discussed above, the concentration of DHA used in our experimental conditions is very low with respect to the concentrations of those usually found to inhibit the growth of tumor cells, even in the bidimensional model [42,61]. The treatment of spheroids with the empty PLGA- or PLGA-TLK-based NPs did not exert any effects on their proliferation. In these experimental conditions, the PLGA-TLK-DTX NPs were only able to slightly (inhibition of 12.1%), but not significantly, inhibit the proliferation of the spheroids. This is in contrast with what was observed in the previous experiment shown in Figure 5, where the bidimensional cell culture conditions were used. However, it should be underlined that in this experiment with spheroids, we decided to evaluate the anticancer effect of the nanoformulations at a lower concentration ($5 \mu\text{L}/\text{mL}$) to avoid the cytotoxic effect of TKL. These results underline the importance of using the 3D culture model when studying the potential anticancer effect of a new compound. Interestingly, however, the PLGA-DTX-DHA NPs were the only ones able to significantly inhibit the spheroid viability (inhibition of 69.5% with respect to control, $p < 0.05$), suggesting that the presence of DHA may substantially increase the anticancer effect of the nanoformulation. The photographs in panel B clearly demonstrate that the treatment with DTX alone is accompanied by the formation of spheroids that are even greater with respect to control spheroids. Moreover, we observed that the concomitant presence of DHA in the PLGA-DTX NPs is able to reduce the number and the volume of tumor spheroids.

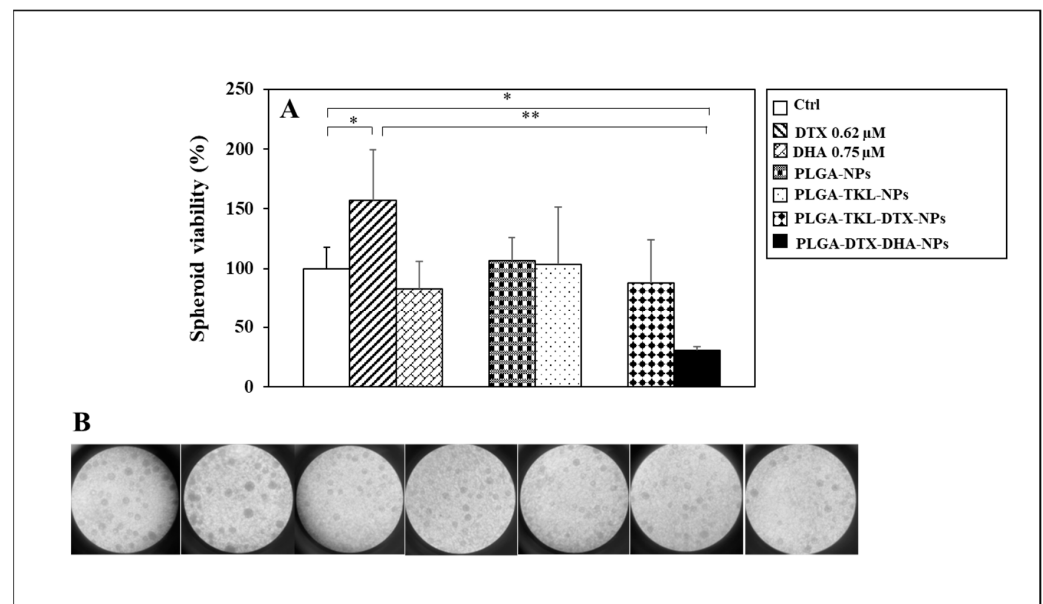


Figure 6. Effect of a 72 h treatment with PLGA-based empty NPs or PLGA-TKL-based empty NPs containing or not 10% DTX (corresponding to $0.62 \mu\text{M}$) or DTX+ DHA (both at 5%, corresponding to $0.31 \mu\text{M}$ and $0.75 \mu\text{M}$, respectively) or with pure DTX ($0.62 \mu\text{M}$) and pure DHA ($0.75 \mu\text{M}$) on the viability of spheroids obtained from HCT116 cells (see the Materials and Methods section for further details). In panel (A), data are the means \pm SD of triplicate values obtained for each experimental condition (*: significantly different, $p < 0.05$; **: significantly different, $p < 0.01$; one-way ANOVA followed by Tukey's test). In panel (B), representative microscope images of the spheroids formed in the different experimental conditions (in the same order as the histogram in panel (A)).

4. Conclusions

Significant advances in the field of oral chemotherapy could lead to a new era of chemotherapy by reducing the number of problems in terms of patient compliance and burden on the healthcare system in the treatment of CRC.

In this study, the aim was the design, realization and study of NPs based on PLGA and TKL, loaded with DTX and DHA, in order to develop a novel, site-specific therapeutic carrier for the treatment of CRC. The NPs showed good encapsulation efficiency, stability and a size suitable for oral administration. Release tests revealed that the encapsulated drugs were released from the NPs within 24 h in quantities ranging from 30 to 35%. Cell viability studies by MTT assay, using a human colon adenocarcinoma cell line (HCT116), revealed a marked inhibition of cell viability by the different DTX-containing NPs and especially when they were co-loaded with DTX and TKL or DHA. Moreover, our data also showed that the presence of DHA allowed us to half the DTX concentration and obtain the same effect, thus reducing the possible side effects of this drug. The use of a 3D culture model of the same tumor cells revealed that also in these conditions, the PLGA-DTX-DHA NPs were efficacious in inhibiting the proliferation of tumor spheroids more than the NPs containing only DTX.

Author Contributions: Conceptualization, R.C., S.T., G.C., S.S., F.C. and R.S.; formal analysis, R.C., S.T., S.S. and G.C.; investigation, R.C., S.T., F.C., R.S. and S.S.; resources, R.C., S.T., G.C. and S.S.; data curation, R.C., S.T., G.C. and S.S.; writing—original draft preparation, R.C., S.T., G.C. and S.S.; writing—review and editing, R.C., S.T., G.C. and S.S.; visualization, R.C., S.T., G.C. and S.S.; supervision, R.C., S.T., G.C. and S.S.; project administration, R.C., S.T., G.C. and S.S.; funding acquisition, R.C., S.T., G.C. and S.S. All authors have read and agreed to the published version of the manuscript.

Funding: This work was supported in part by the Department of Pharmacy and Health and Nutrition Sciences. Department of Excellence L. 232/2016 and by PON R&I 2014-2020—ARS01_00568—SI.F.I.PA.CRO.DE.—Development and Industrialization of Innovative Drugs for Personalized Molecular Therapy PA.CRO.DE. and in part by grants Linea D1 2021 to G.C. and Linea D1 2022 to S.S. from Università Cattolica del S. Cuore.

Institutional Review Board Statement: Not applicable.

Informed Consent Statement: Not applicable.

Data Availability Statement: The datasets analyzed during the current study are available from the corresponding author on reasonable request.

Conflicts of Interest: The authors declare no conflicts of interest.

References

1. Rawla, P.; Sunkara, T.; Barsouk, A. Epidemiology of colorectal cancer: Incidence, mortality, survival, and risk factors. *Gastroenterol. Rev.* **2019**, *14*, 89–103. [[CrossRef](#)]
2. Sheikh-Wu, S.F.; Anglade, D.; Gattamorta, K.; Downs, C.A. Relationships Between Colorectal Cancer Survivors' Positive Psychology, Symptoms, and Quality of Life. *Clin. Nurs. Res.* **2023**, *32*, 171–184. [[CrossRef](#)]
3. Dekker, E.; Tanis, P.J.; Vleugels, J.L.A.; Kasi, P.M.; Wallace, M.B. Colorectal cancer. *Lancet* **2019**, *394*, 1467–1480. [[CrossRef](#)]
4. Punt, C.J.; Koopman, M.; Vermeulen, L. From tumour heterogeneity to advances in precision treatment of colorectal cancer. *Nat. Rev. Clin. Oncol.* **2017**, *14*, 235–246. [[CrossRef](#)]
5. Gustavsson, B.; Carlsson, G.; Machover, D.; Petrelli, N.; Roth, A.; Schmoll, H.J.; Tveit, K.M.; Gibson, F. A review of the evolution of systemic chemotherapy in the management of colorectal cancer. *Clin. Colorectal Cancer* **2015**, *14*, 1–10. [[CrossRef](#)]
6. Ying, K.; Bai, B.; Gao, X.; Xu, Y.; Wang, H.; Xie, B. Orally administrable therapeutic nanoparticles for the treatment of colorectal cancer. *Frontiers in Bioengineering and Biotechnology. Front. Bioeng. Biotechnol.* **2021**, *9*, 670124. [[CrossRef](#)]
7. Zhang, X.; Song, H.; Canup, B.S.B.; Xiao, B. Colorectal Cancer immunotherapy: Options and strategies. *Expert Opin. Drug Delivery* **2020**, *17*, 781–790. [[CrossRef](#)]
8. Wong, A.H.N.; Ma, B.; Lui, R.N. New developments in targeted therapy for metastatic colorectal cancer. *Ther. Adv. Med. Oncol.* **2023**, *15*, 17588359221148540. [[CrossRef](#)]

9. Ünal, S.; Aktaş, Y.; Benito, J.M.; Bilensoy, E. Cyclodextrin nanoparticle bound oral camptothecin for colorectal cancer: Formulation development and optimization. *Int. J. Pharm.* **2020**, *584*, 119468. [[CrossRef](#)]
10. Ünal, S.; Öztürk, S.C.; Bilgiç, E.; Yanık, H.; Korkusuz, P.; Aktaş, Y.; Benito, J.M.; Esendağlı, G.; Bilensoy, E. Therapeutic efficacy and gastrointestinal biodistribution of polycationic nanoparticles for oral camptothecin delivery in early and late-stage colorectal tumor-bearing animal model. *Eur. J. Pharm. Biopharm.* **2021**, *169*, 168–177. [[CrossRef](#)]
11. Cabeza, L.; Perazzoli, G.; Mesas, C.; Jiménez-Luna, C.; Prados, J.; Rama, A.R.; Melguizo, C. Nanoparticles in Colorectal Cancer Therapy: Latest In Vivo Assays, Clinical Trials, and Patents. *AAPS PharmSciTech* **2020**, *21*, 178. [[CrossRef](#)]
12. Pardeshi, S.R.; Nikam, A.; Chandak, P.; Mandale, V.; Naik, J.B.; Giram, P.S. Recent advances in PLGA based nanocarriers for drug delivery system: A state of the art review. *Int. J. Polym. Mater. Polym. Biomater.* **2023**, *72*, 49–78. [[CrossRef](#)]
13. Pereira, S.; Egbu, R.; Jannati, G.; Al-Jamal, W.T. Docetaxel-loaded liposomes: The effect of lipid composition and purification on drug encapsulation and in vitro toxicity. *Int. J. Pharm.* **2016**, *514*, 150–159. [[CrossRef](#)]
14. Kim, S.M.; Lee, S.Y.; Yuk, D.Y.; Moon, D.C.; Choi, S.S.; Kim, Y.; Han, S.B.; Oh, K.W.; Hong, J.T. Inhibition of NF-kappaB by ginsenoside Rg3 enhances the susceptibility of colon cancer cells to docetaxel. *Arch. Pharm. Res.* **2009**, *32*, 755–765. [[CrossRef](#)]
15. Han, T.D.; Shang, D.H.; Tian, Y. Docetaxel enhances apoptosis and G2/M cell cycle arrest by suppressing mitogen-activated protein kinase signaling in human renal clear cell carcinoma. *Genet. Mol. Res.* **2016**, *15*, 1. [[CrossRef](#)]
16. Sternberg, C.N.; ten Bokkel Huinink, W.W.; Smyth, J.F.; Brunsch, V.; Dirix, L.Y.; Pavlidis, N.A.; Franklin, H.; Wanders, S.; Le Bail, N.; Kaye, S.B. Docetaxel (Taxotere), a novel taxoid, in the treatment of advanced colorectal carcinoma: An EORTC Early Clinical Trials Group Study. *Br. J. Cancer* **1994**, *70*, 376–379. [[CrossRef](#)]
17. Pazdur, R.; Lassere, Y.; Soh, L.T.; Ajani, J.A.; Bready, B.; Soo, E.; Sugarman, S.; Patt, Y.; Abbruzzese, J.L.; Levin, B. Phase II trial of docetaxel (Taxotere) in metastatic colorectal carcinoma. *Ann. Oncol.* **1994**, *5*, 468–470. [[CrossRef](#)]
18. Ünal, S.; Doğan, O.; Aktaş, Y. Orally administered docetaxel-loaded chitosan-decorated cationic PLGA nanoparticles for intestinal tumors: Formulation, comprehensive in vitro characterization, and release kinetics. *Beilstein J. Nanotechnol.* **2022**, *13*, 1393–1407. [[CrossRef](#)]
19. Gu, Z.; Da Silva, C.G.; Hao, Y.; Schomann, T.; Camps, M.G.M.; van der Maaden, K.; Liu, Q.; Ossendorp, F.; Cruz, L.J. Effective combination of liposome-targeted chemotherapy and PD-L1 blockade of murine colon cancer. *J. Control. Release* **2023**, *353*, 490–506. [[CrossRef](#)]
20. Wang, C.; Aguilar, A.; Ojima, I. Strategies for the drug discovery and development of taxane anticancer therapeutics. *Expert Opin. Drug Discov.* **2022**, *17*, 1193–1207. [[CrossRef](#)]
21. Zou, Y.; Xiao, F.; Song, L.; Sun, B.; Sun, D.; Chu, D.; Wang, L.; Han, S.; Yu, Z.; O'Driscoll, C.M.; et al. A folate-targeted PEGylated cyclodextrin-based nanoformulation achieves co-delivery of docetaxel and siRNA for colorectal cancer. *Int. J. Pharm.* **2021**, *606*, 120888. [[CrossRef](#)]
22. Wang, C.; Wang, J.; Zhang, X.; Yu, S.; Wen, D.; Hu, Q.; Ye, Y.; Bomba, H.; Hu, X.; Liu, Z.; et al. In situ formed reactive oxygen species-responsive scaffold with gemcitabine and checkpoint inhibitor for combination therapy. *Sci. Transl. Med.* **2018**, *10*, eaan3682. [[CrossRef](#)]
23. Shekari, N.; Javadian, M.; Ghasemi, M.; Baradaran, B.; Darabi, M.; Kazemi, T. Synergistic Beneficial Effect of Docosahexaenoic Acid (DHA) and Docetaxel on the Expression Level of Matrix Metalloproteinase-2 (MMP-2) and MicroRNA-106b in Gastric Cancer. *J. Gastrointest. Cancer* **2020**, *51*, 70–75. [[CrossRef](#)]
24. Newell, M.; Goruk, S.; Mazurak, V.; Postovit, L.; Field, C.J. Role of docosahexaenoic acid in enhancement of docetaxel action in patient-derived breast cancer xenografts. *Breast Cancer Res. Treat.* **2019**, *177*, 357–367. [[CrossRef](#)]
25. Dong, P.; Liu, J.; Lv, H.; Wu, J.; Zhang, N.; Wang, S.; Li, X.; Hu, J.; Wang, A.; Li, D.J.; et al. The enhanced antitumor activity of the polymeric conjugate covalently coupled with docetaxel and docosahexaenoic acid. *Biomater. Sci.* **2022**, *10*, 3454–3465. [[CrossRef](#)]
26. Shao, Z.C.; Zhu, B.H.; Huang, A.F.; Su, M.Q.; An, L.J.; Wu, Z.P.; Jiang, Y.J.; Guo, H.; Han, X.Q.; Liu, C.M. Docosahexaenoic Acid Reverses Epithelial-Mesenchymal Transition and Drug Resistance by Impairing the PI3K/AKT/Nrf2/GPX4 Signalling Pathway in Docetaxel-Resistant PC3 Prostate Cancer Cells. *Folia Biol.* **2022**, *68*, 59–71. [[CrossRef](#)]
27. Siddiqui, R.A.; Harvey, K.A.; Xu, Z.; Bammerlin, E.M.; Walker, C.; Altenburg, J.D. Docosahexaenoic acid: A natural powerful adjuvant that improves efficacy for anticancer treatment with no adverse effects. *Biofactors* **2011**, *37*, 399–412. [[CrossRef](#)]
28. Corsetto, P.A.; Colombo, I.; Kopecka, J.; Rizzo, A.M.; Riganti, C. ω -3 Long Chain Polyunsaturated Fatty Acids as Sensitizing Agents and Multidrug Resistance Revertants in Cancer Therapy. *Int. J. Mol. Sci.* **2017**, *18*, 2770. [[CrossRef](#)]
29. Giordano, C.; Plastina, P.; Barone, I.; Catalano, S.; Bonfiglio, D. *n*-3 Polyunsaturated Fatty Acid Amides: New Avenues in the Prevention and Treatment of Breast Cancer. *Int. J. Mol. Sci.* **2020**, *21*, 2279. [[CrossRef](#)]
30. Chen, J.; Zaal, E.A.; Berkers, C.R.; Ruijtenbeek, R.; Garssen, J.; Redegeld, F.A. Omega-3 Fatty Acids DHA and EPA Reduce Bortezomib Resistance in Multiple Myeloma Cells by Promoting Glutathione Degradation. *Cells* **2021**, *10*, 2287. [[CrossRef](#)]
31. Liu, Y.; Tian, Y.; Guo, Y.; Yan, Z.; Xue, C.; Wang, J. DHA-enriched phosphatidylcholine suppressed angiogenesis by activating PPAR γ and modulating the VEGFR2/Ras/ERK pathway in human umbilical vein endothelial cells. *Food Sci. Biotechnol.* **2021**, *30*, 1543–1553. [[CrossRef](#)]
32. Fodil, M.; Blanckaert, V.; Ulmann, L.; Mimouni, V.; Chénais, B. Contribution of *n*-3 Long-Chain Polyunsaturated Fatty Acids to the Prevention of Breast Cancer Risk Factors. *Int. J. Environ. Res. Public Health* **2022**, *19*, 7936. [[CrossRef](#)]

33. Sasazuki, S.; Inoue, M.; Iwasaki, M.; Sawada, N.; Shimazu, T.; Yamaji, T.; Takachi, R.; Tsugane, S. Intake of n-3 and n-6 polyunsaturated fatty acids and development of colorectal cancer by subsite: Japan Public Health Center-based prospective study. *Int. J. Cancer* **2011**, *129*, 1718–1729. [[CrossRef](#)]
34. Murff, H.J.; Shrubsole, M.J.; Cai, Q.; Smalley, W.E.; Dai, Q.; Milne, G.L.; Ness, R.M.; Zheng, W. Dietary intake of PUFAs and colorectal polyp risk. *Am. J. Clin. Nutr.* **2012**, *95*, 703–712. [[CrossRef](#)]
35. Kim, S.; Sandler, D.P.; Galanko, J.; Martin, C.; Sandler, R.S. Intake of polyunsaturated fatty acids and distal large bowel cancer risk in whites and African Americans. *Am. J. Epidemiol.* **2010**, *171*, 969–979. [[CrossRef](#)]
36. Hall, M.N.; Chavarro, J.E.; Lee, I.M.; Willett, W.C.; Ma, J. A 22-year prospective study of fish, n-3 fatty acid intake, and colorectal cancer risk in men. *Cancer Epidemiol. Biomarkers Prev.* **2008**, *17*, 1136–1143. [[CrossRef](#)] [[PubMed](#)]
37. Pot, G.K.; Geelen, A.; van Heijningen, E.M.; Siezen, C.L.; van Kranen, H.J.; Kampman, E. Opposing associations of serum n-3 and n-6 polyunsaturated fatty acids with colorectal adenoma risk: An endoscopy-based case-control study. *Int. J. Cancer* **2008**, *123*, 1974–1977. [[CrossRef](#)]
38. Calviello, G.; Resci, F.; Serini, S.; Piccioni, E.; Toesca, A.; Boninsegna, A.; Monego, G.; Ranelletti, F.O.; Palozza, P. Docosahexaenoic acid induces proteasome-dependent degradation of beta-catenin, down-regulation of survivin and apoptosis in human colorectal cancer cells not expressing COX-2. *Carcinogenesis* **2007**, *28*, 1202–1209. [[CrossRef](#)]
39. Fasano, E.; Serini, S.; Piccioni, E.; Toesca, A.; Monego, G.; Cittadini, A.R.; Ranelletti, F.O.; Calviello, G. DHA induces apoptosis by altering the expression and cellular location of GRP78 in colon cancer cell lines. *Biochim. Biophys. Acta* **2012**, *1822*, 1762–1772. [[CrossRef](#)] [[PubMed](#)]
40. Serini, S.; Cassano, R.; Corsetto, P.A.; Rizzo, A.M.; Calviello, G.; Trombino, S. Omega-3 PUFA Loaded in Resveratrol-Based Solid Lipid Nanoparticles: Physicochemical Properties and Antineoplastic Activities in Human Colorectal Cancer Cells In Vitro. *Int. J. Mol. Sci.* **2018**, *19*, 586. [[CrossRef](#)]
41. Trombino, S.; Serini, S.; Cassano, R.; Calviello, G. Xanthan gum-based materials for omega-3 PUFA delivery: Preparation, characterization and antineoplastic activity evaluation. *Carbohydr. Polym.* **2019**, *208*, 431–440. [[CrossRef](#)] [[PubMed](#)]
42. Calviello, G.; Di Nicuolo, F.; Serini, S.; Piccioni, E.; Boninsegna, A.; Maggiano, N.; Ranelletti, F.O.; Palozza, P. Docosahexaenoic acid enhances the susceptibility of human colorectal cancer cells to 5-fluorouracil. *Cancer Chemother. Pharmacol.* **2005**, *55*, 12–20. [[CrossRef](#)] [[PubMed](#)]
43. Calviello, G.; Di Nicuolo, F.; Gragnoli, S.; Piccioni, E.; Serini, S.; Maggiano, N.; Tringali, G.; Navarra, P.; Ranelletti, F.O.; Palozza, P. n-3 PUFAs reduce VEGF expression in human colon cancer cells modulating the COX-2/PGE2 induced ERK-1 and -2 and HIF-1alpha induction pathway. *Carcinogenesis* **2004**, *25*, 2303–2310. [[CrossRef](#)] [[PubMed](#)]
44. ten Tije, A.J.; Verweij, J.; Loos, W.J.; Sparreboom, A. Pharmacological effects of formulation vehicles: Implications for cancer chemotherapy. *Clin. Pharmacokinet.* **2003**, *42*, 665–685. [[CrossRef](#)] [[PubMed](#)]
45. van Zuylen, L.; Verweij, J.; Sparreboom, A. Role of formulation vehicles in taxane pharmacology. *Investig. New Drugs* **2001**, *19*, 125–141. [[CrossRef](#)]
46. Chiu, H.I.; Lim, V. Wheat Germ Agglutinin-Conjugated Disulfide Cross-Linked Alginate Nanoparticles as a Docetaxel Carrier for Colon Cancer Therapy. *Int. J. Nanomed.* **2021**, *16*, 2995–3020. [[CrossRef](#)]
47. Freitas, R.D.S.; Campos, M.M. Protective Effects of Omega-3 Fatty Acids in Cancer-Related Complications. *Nutrients* **2019**, *11*, 945. [[CrossRef](#)] [[PubMed](#)]
48. Yoon, S.L.; Grundmann, O. Relevance of Dietary Supplement Use in Gastrointestinal-Cancer-Associated Cachexia. *Nutrients* **2023**, *15*, 3391. [[CrossRef](#)]
49. Liou, G.Y.; Storz, P. Reactive oxygen species in cancer. *Free Radic. Res.* **2010**, *44*, 479–496. [[CrossRef](#)]
50. Li, C.; Wei, Y.; Xue, C.; Chen, M.; Fei, Y.; Tan, L.; Luo, Z.; Cai, K.; Hu, Y. ROS-activatable biomimetic interface mediates in-situ bioenergetic remodeling of osteogenic cells for osteoporotic bone repair. *Biomaterials* **2022**, *291*, 121878.
51. Brancato, V.; Oliveira, J.M.; Correló, V.M.; Reis, R.L.; Kundu, S.C. Could 3D models of cancer enhance drug screening? *Biomaterials* **2020**, *232*, 119744. [[CrossRef](#)]
52. Cassano, R.; Curcio, F.; Procopio, D.; Fiorillo, M.; Trombino, S. Multifunctional Microspheres Based on D-Mannose and Resveratrol for Ciprofloxacin Release. *Materials* **2022**, *15*, 7293. [[CrossRef](#)]
53. Trombino, S.; Malivindi, R.; Barbarossa, G.; Sole, R.; Curcio, F.; Cassano, R. Solid Lipid Nanoparticles Hydroquinone-Based for the Treatment of Melanoma: Efficacy and Safety Studies. *Pharmaceutics* **2023**, *15*, 1375. [[CrossRef](#)] [[PubMed](#)]
54. da Silva Feltrin, F.; Agner, T.; Sayer, C.; Ferrareso Lona, L.M. Curcumin encapsulation in functional PLGA nanoparticles: A promising strategy for cancer therapies. *Adv. Colloid Inter. Sci.* **2022**, *300*, 102582. [[CrossRef](#)]
55. Al-Nemrawi, N.K.; Altawabeyeh, R.M.; Darweesh, R.S. Preparation and Characterization of Docetaxel-PLGA Nanoparticles Coated with Folic Acid-chitosan Conjugate for Cancer Treatment. *J. Pharm. Sci.* **2022**, *111*, 485–494. [[CrossRef](#)]
56. Kumar, P.; Nagarajan, A.; Uchil, P.D. Analysis of Cell Viability by the MTT Assay. *Cold Spring Harb. Protoc.* **2018**, *2018*, pdb.prot095505. [[CrossRef](#)] [[PubMed](#)]
57. Hernández-Giottonini, K.Y.; Rodríguez-Córdova, R.J.; Gutiérrez-Valenzuela, C.A.; Peñuñuri-Miranda, O.; Zavala-Rivera, P.; Guerrero-Germán, P.; Lucero-Acuña, A. PLGA nanoparticle preparations by emulsification and nanoprecipitation techniques: Effects of formulation parameters. *RSC Adv.* **2020**, *10*, 4218–4231. [[CrossRef](#)]
58. Xu, A.P.; Xu, L.B.; Smith, E.R.; Fleishman, J.S.; Chen, Z.S.; Xu, X.X. Cell death in cancer chemotherapy using taxanes. *Front. Pharmacol.* **2024**, *14*, 1338633. [[CrossRef](#)] [[PubMed](#)]

59. Kingston, D.G. Tubulin-interactive natural products as anticancer agents. *J. Nat. Prod.* **2009**, *72*, 507–515. [[CrossRef](#)] [[PubMed](#)]
60. Chen, Q.H. Crosstalk between Microtubule Stabilizing Agents and Prostate Cancer. *Cancers* **2023**, *15*, 3308. [[CrossRef](#)]
61. Jin, H.; Kim, H.S.; Yu, S.T.; Shin, S.R.; Lee, S.H.; Seo, G.S. Synergistic anticancer effect of docosahexaenoic acid and isoliquiritigenin on human colorectal cancer cells through ROS-mediated regulation of the JNK and cytochrome c release. *Mol. Biol. Rep.* **2021**, *48*, 1171–1180. [[CrossRef](#)] [[PubMed](#)]
62. Perillo, B.; Di Donato, M.; Pezone, A.; Di Zazzo, E.; Giovannelli, P.; Galasso, G.; Castoria, G.; Migliaccio, A. ROS in cancer therapy: The bright side of the moon. *Exp. Mol. Med.* **2020**, *52*, 192–203. [[CrossRef](#)] [[PubMed](#)]

Disclaimer/Publisher’s Note: The statements, opinions and data contained in all publications are solely those of the individual author(s) and contributor(s) and not of MDPI and/or the editor(s). MDPI and/or the editor(s) disclaim responsibility for any injury to people or property resulting from any ideas, methods, instructions or products referred to in the content.